*Int. J. Electrochem. Sci.*, 15 **(2020)** 710 – 721, doi: 10.20964/2020.01.48

International Journal of
ELECTROCHEMICAL
SCIENCE
www.electrochemsci.org

# Effect of Content of Graphene on Corrosion Behavior of Micro-Arc Oxidation Coating on Titanium Alloy Drill Pipe

*Xiaowen Chen*[*], *Dandan Liao, Defen Zhang, Xuan Jiang, Pengfei Zhao, Ruosi Xu*

School of Materials Science and Engineering, Southwest Petroleum University, Chengdu 610500, China
[*]E-mail: xwchen5188@163.com

*Received:* 17 September 2019 / *Accepted:* 4 November 2019 / *Published:* 30 November 2019

---

To improve the corrosion resistance of titanium alloy drill pipe, graphene particles was added into the electrolyte and micro-arc oxidation composite coating was formed with different graphene contents on the surface of TC4 titanium alloy. The corrosion characteristics of titanium alloy micro-arc oxidation film were analyzed by electrochemical workstation. The galvanic corrosion performance between TC4 titanium alloy and S135 steel was measured by galvanic corrosion tester. Results showed that on the surface of TC4 titanium alloy after micro-arc oxidation treatment, there is a dense oxide coating with good stability and high electrical resistance, which can effectively stabilize and reduce the galvanic current, so the coupling of micro-arc oxidation coating and S135 steel after galvanic pairing the current is significantly reduced. Micro-arc oxidation treatment of titanium alloy can improve surface corrosion resistance and reduce galvanic corrosion sensitivity. It is also found that the optimum graphene addition is 3 g/L under the experimental conditions.

---

**Keywords:** Titanium alloy; Electrochemical; Galvanic corrosion; Micro-arc oxidation; Graphene additive

## 1. INTRODUCTION

Titanium and titanium alloys are used as common materials of high-performance structural parts which also are called "ocean metal" or "space metal" due to their excellent mechanical properties and corrosion resistance[1,2]. Furthermore, titanium alloys are widely used in medical equipments, chemical industries and aerospaces because of excellent biocompatibility, hydrogen storage, superconductivity, shape memory and other special functions[3]. In the oil industry, titanium alloys are mainly used in the construction of deep wells and large displacement wells on account of high safety of titanium alloy drill pipe[4-6]. Nonetheless, the conditions are more complicated in the actual environment, parts are required to work under various harsh and extreme conditions such as high temperature and high pressure environment, acidic medium or dissimilar metal contact. However, titanium alloys have a higher positive potential than other alloys, and are protected as cathodes when coupled with dissimilar alloys, accelerating the corrosion of the even bond gold which can result in structural failure[7]. Therefore, we need surface treatment of titanium alloy to improve the safety and service life of parts.

In the galvanic corrosion test of oil well pipe in the downhole corrosive environment, Xing [8,9] researched the galvanic corrosion law between 3Cr, 9Cr, 13Cr and Super13Cr and found that the effect of steel grade on galvanic corrosion is little, and the use of transition material is advantageous to the protection of low chromium alloy and prolongs its service life. Research from Chen [10] showed that when T2 alloy acts as anode and TC4 alloy acts as cathode, the corrosion rate increases and the release rate of galvanic corrosion copper ions is significantly improved, maintaining at 160 $\mu g/(cm^2 \cdot d)$ in the galvanic corrosion test of T2/TC4 galvanic couple in static artificial seawater. Chen [11] reported that after micro-arc oxidation treatment on the titanium alloy drill pipe by adding sodium tungstate to the electrolyte, it is found that the galvanic corrosion acceleration coefficient of the oxide coating and the S135 steel galvanic couple is significantly lower than that of the titanium alloy substrate. Palani [12] studied galvanic corrosion between 3 materials, carbon fibre composite and aluminium alloy joined with titanium fastener,using thin flm approach. Snihirova [13] focuses on the development of a physico-chemical model based on mechanistic and kinetics understanding of the corrosion process in galvanic couple Ti6Al4V-AA2024. Yang [14,15] studied the susceptibility to galvanic corrosion between of TC4-DT titanium alloy and dissimilar material such as aluminum alloys, steels and their anodized. The results indicated that anodizing titanium alloy and aluminum alloy can effectively reduce the sensitivity of electric contact corrosion and has better protection effect. In order to further improve the surface properties of titanium alloy drill pipe and expand its application prospect in the field of oil and gas. Chen [16] studied the galvanic corrosion behavior of stainless steel (17-4) and carbon steel (C110), and found that the passivation coating on 17-4 stainless steel is unstable due to cathodic polarization in the galvanic couple. The research from Du [17] demonstrate that EN 6061 T6/hot-galvanized IF steel subject to tox punching presented more severe galvanic corrosion than the self-piercing rivet joint. In this work, TC4 titanium alloy was used as the base material, we study on galvanic corrosion performance of TC4 titanium alloy micro-arc oxidation coating (MAO) which prepared with different graphene contents and S135 drill pipe. To further improve the surface properties of titanium alloy drill pipe, expand its application prospect in the field of oil and gas, and provide scientific basis for the practical application of titanium alloy drill pipe.

## 2. EXPERIMENTAL

### *2.1. Materials preparation*

The materials used in this work were TC4 titanium alloy and S135 carbon steel, with the compositions listed in Table 1. The cutting size of the sample was 40 mm×20 mm×4 mm. After the oil stain was removed by acetone, all specimens were successfully polished with 400#, 800#, 1000# and 1500# SiC papers, followed by an ultrasonic cleaning in alcohol. It was then dried and sealed for use.

**Table 1.** Chemical compositions (wt. %) of metals used in this work

| Material | C | V | Si | Mn | P | S | Cr | Mo | Ni | Al | H | O | Fe | Ti |
|---|---|---|---|---|---|---|---|---|---|---|---|---|---|---|
| **S135** | 0.37 | 0.013 | 0.25 | 0.65 | 0.012 | 0.007 | 0.25 | 0.22 | 0.017 | - | - | - | Bal. | 0.04 |
| **TC4** | ≤0.1 | 3.5~4.5 | - | - | - | - | - | - | - | 5.5~6.8 | ≤0.015 | ≤0.2 | ≤0.3 | Bal. |

### *2.2. Preparation of MAO coating*

The titanium alloy samples were treated by microarc oxidation with DWL20-6 pulse DC micro-arc oxidation device (Produced in Institute of Surface Science and Engineering Technology, Xihua University). According to the basis of previous relevant experimental results, the MAO parameters were as follows: frequency is 100 Hz, duty ratio 60%, current density is 6 A/dm$^2$ and oxidation time is 30 min. The base electrolyte used for MAO was composed of $Na_2SiO_3 \cdot 9H_2O$ (8 g/L), $(NaPO_3)_6 \cdot 6H_2O$ (4 g/L) and $C_3H_8O_3$ (4 mL/L). Graphene particles with slice size of 10~20 μm was added into the base electrolyte and dispersed by mechanical stirring. The samples with graphene concentration of 0 g/L, 0.5 g/L, 3 g/L and 6 g/L were named as G0, G0.5, G3 and G6, respectively. During the micro-arc oxidation processing, the electrolyte temperature was held no more than 35 °C by the cooling system.

The surface morphology and cross-section of the micro-arc oxidation coating were observed using a ZEISS EVOMA15 scanning electron microscope (SEM). Phase composition of the MAO coatings was investigated by X-ray diffraction (DX-2700B), use copper target Kα ray, tube voltage and current is 40 kV and 30 mA, respectively. Continuous scanning diffraction angle is 10°～90°, step size is 0.02°, 0.5 s per step.

### *2.3. Electrochemical experiments*

In the galvanic corrosion test of the TC4/S135 galvanic pair, the galvanic pair distance is 10 mm, and the area ratio of TC4 to S135 is 1:1. The test is carried out according to the standard GB/T 15748-2013, the corrosive medium is 3.5% chloride solution with pH value is 7, and at the test temperature of 35 °C, the test lasted for 10 h. The electrode potential was the open circuit potential after the sample was stabilized for 0.5 h in the corrosive solution. It was used to determine the polarity of the galvanic couple and determine the direction of the galvanic current.

The saturated calomel electrode is used as the reference electrode, and the corrosion performance of the graphene-modified micro-arc oxidation coating is measured by ZRA-2 galvanic corrosion measuring instrument. Using the timing acquisition and recording data, the value of the coupling current and the coupling voltage is recorded once every half hour. To ensure the reproducibility, each type of electrochemical measurements is repeated at least three times. The electrochemical tests, including open circuit potential (OCP), galvanic potential, potentidynamic polarization and electrochemical impedance spectroscopy (EIS) were conducted by a IM6 electrochemical workstation with a three-electrode system (which with a platinum electrode as the auxiliary electrode, a saturated calomel electrode as the reference electrode, and a TC4 and S135 sample as the working electrode). Dynamic potential polarization curve test parameters: scan range is -500 ~ +1000 mV (relative to open circuit potential), scanning rate is 1 mV/s. In the electrochemical impedance test, test frequency range is 50 mHz~100 kHz, voltage amplitude is 5 mV.

## 3. RESULTS AND DISCUSSION

### *3.1. Effect of graphene content on coating properties*

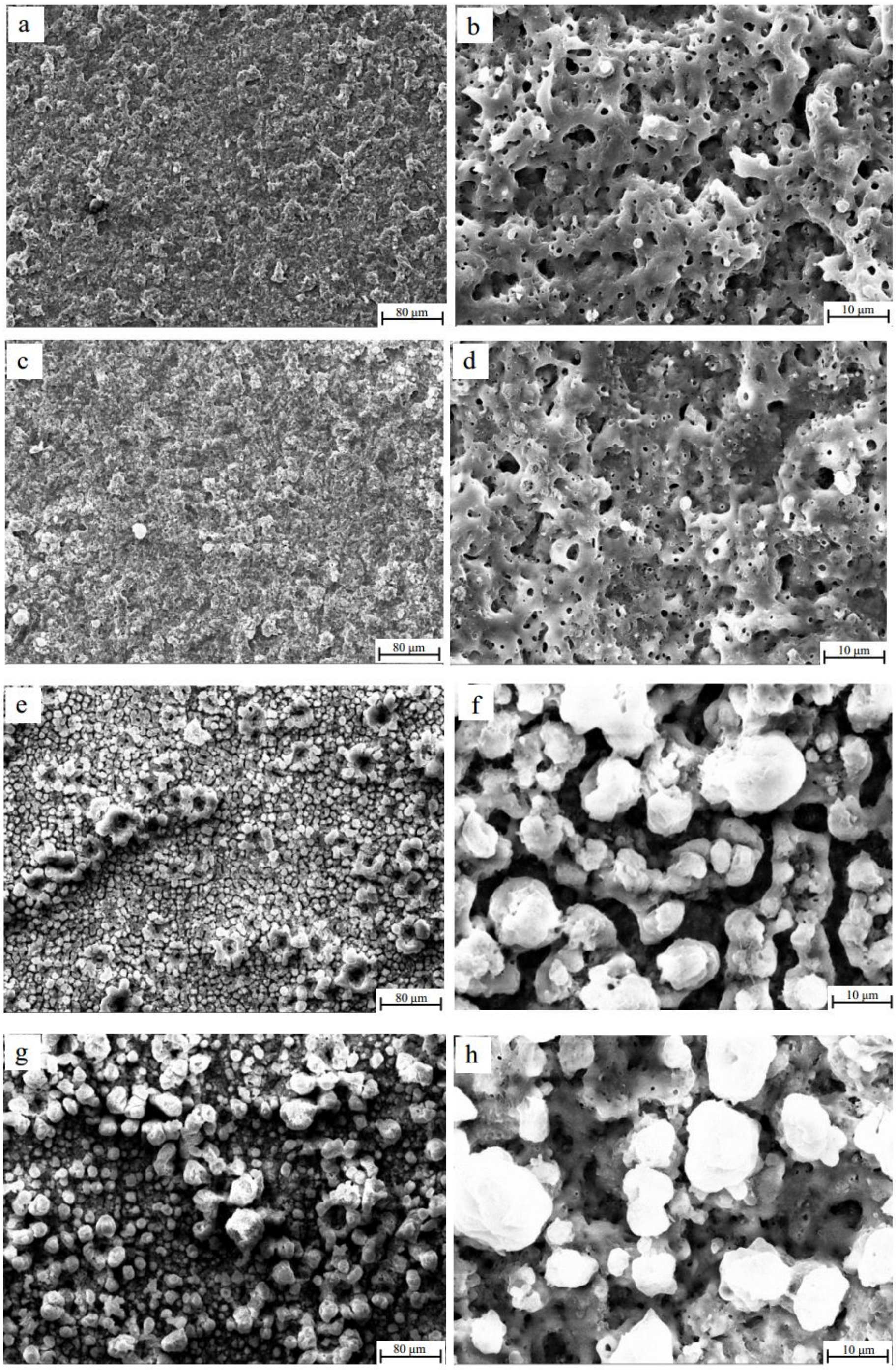

**Figure 1.** Surface morphology of coating samples after 30 minutes of micro-arc oxidation treatment: (a,b) without graphene ; (c,d) with 0.5 g/L graphene ; (e,f) with 3 g/L graphene ; (g,h) with 6 g/L graphene

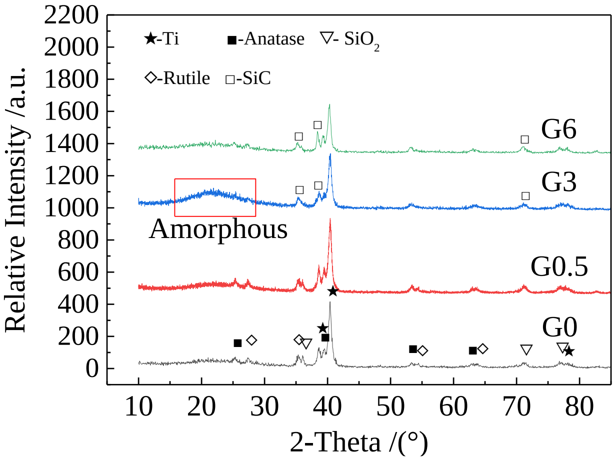

**Figure 2.** Influence of graphene concentration on XRD patterns of different coating samples G0-without graphene; G0.5-with 0.5 g/L graphene ; G3-with 3 g/L graphene ; G6-with 6 g/L graphene

Figure 1 shows the surface morphology of the micro-arc oxide coating. It can be seen the coating has a porous structure and and the surface is composed of coarse and uneven particles, there are residual discharge pores of different sizes in the middle of each large particle with diameter range from 1 to 5μm, the pore shape is similar to the crater. Under the intense action of the flare discharge, a large amount of melt is generated in the arc discharge channel. Rapid solidification crystallization under the rapid cooling of the electrolyte, and the reaction product in the channel also cools and shrinks. Thereby, the particles are melted and then stacked together, and the molten tissue and the voids cover each other to form a residual morphology similar to that after the volcanic eruption. It is found that with the increased graphene content from 0 to 6 g/L, both the coating roughness and diameter of discharge micropores increased. The main reason is that graphene is a strong conductive material, and the conductivity of the electrolyte is enhanced after the addition of graphene, resulting in a more intense reaction process.

The phase composition of the coating is shown in Figure 2. It can be found that the coatings are mainly composed of anatase $TiO_2$ and rutile $TiO_2$. The rutile phase and the anatase phase are two different phase structures of titanium dioxide. At higher temperatures, the metastable anatase phase can be easily converted into a stable rutile phase. The elements in the solution also participate in the formation of the oxide coating. The crystal phase of the P and Si elements is not detected. It may be that Si and P elements exist in the amorphous form in the oxide coating. The content of graphene particles entering the oxide coating is extremely small, and it is difficult to find the diffraction peak of graphene in the XRD diffraction results. As the graphene content increases, the micro-arc oxidation process becomes more intense, and some graphene reacts with the coating and forms SiC under the influence of high temperature. During the formation of the amorphous alloy, the molten liquid is rapidly cooled [18], and the atoms are not properly aligned during the cooling process to form an amorphous metastable state.

### *3.2. Effect of graphene content on electrochemical behavior of coating*

Figure 3 shows the potentiodynamic polarization curve in the simulated etching solution of TC4 titanium alloy micro-arc oxidation coating. The electrochemical parameters obtained by fitting the polarization curve of Fig. 3 using the Tafel extrapolation method are shown in Table 2. With the increase of graphene content, the self-corrosion potential of the composite coating first increases and then decreases. When the graphene content is 3 g/L, the self-corrosion potential of the micro-arc oxidation composite coating is up to 0.403 V. The corrosion current density is at least $2.66\times10^{-9}$ A/cm$^2$, and the corrosion resistance is the best. Compared with the titanium alloy matrix, the corrosion potential of the MAO coating is significantly increased. The corrosion resistance of the coating has been further improved after the addition of graphene.

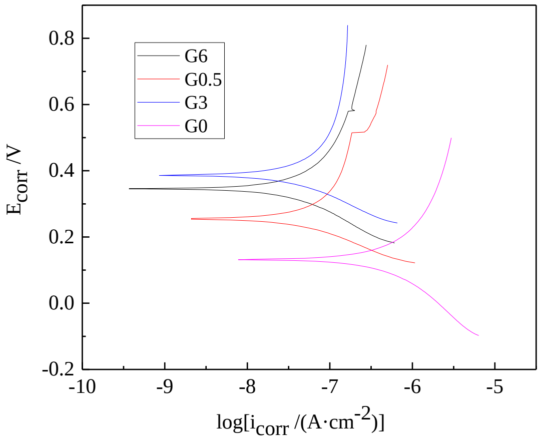

**Figure 3** Influence of graphene concentration on Potentiodynamic polarization curves for MAO coating samples

The polarization resistance $R_P$ and the corrosion rate $C_R$ are calculated by the Stern-Geary equation [19] as shown in Eq.( 1, 2):

$$R_P = \frac{\beta_a \cdot \beta_c}{2.3 \cdot i_{corr}(\beta_a + \beta_c)} \qquad (1)$$

$$C_R = 22.85 i_{corr} \qquad (2)$$

Where $\beta_a$ represents the slope of the anode and $\beta_c$ represents the slope of the cathode.

Table 2 shows the polarization resistance and corrosion rate after electrochemical corrosion of samples. The results indicate that with the addition of graphene particles, the polarization resistance of the coatings increases and the corrosion rate decreases. Corrosion rate in galvanic corrosion reactions depends not only on dissimilar metals potential difference between each other but also affected by polarization resistance. When the graphene content is 3 g/L, the coating has the best corrosion performance, owing to polarization resistance reached a maximum of $1.78\times10^{7}$ Ω•cm$^2$ and corrosion rate reached a minimum of $6.1\times10^{-8}$ A/cm$^2$. This indicates that in this study, the decrease in galvanic potential is mainly caused by the increase in the Tafel slope of the polarization curve of the titanium alloy constituting the galvanic cathode after micro-arc oxidation. The decrease in corrosion current density $I_{corr}$ in Table 2 and the increase in film resistance $R_p$ in Table 3 also confirmed that the addition of graphene increased in the micro-arc oxidation of titanium alloy, and the Tafel slope increased. Therefore, combined with the results of polarization curve test and AC impedance, it can be seen that the decrease of galvanic corrosion current density caused by micro-arc oxidation of titanium alloy is mainly due to the increase of electrochemical coating resistance of titanium alloy after micro-arc oxidation.

**Table 2.** Electrochemical parameters of samples in 3.5% sodium chloride solution

| Sample | $i_{corr}$ /A·cm$^{-2}$ | $E_{corr}$ /V | $\beta_a$（V/dec） | -$\beta_c$（V/dec） | $R_p$（Ω•cm$^2$） | $C_R$（A/cm$^2$） |
|---|---|---|---|---|---|---|
| G0 | $4.34\times10^{-7}$ | 0.132 | 0.273 | 0.197 | $1.15\times10^{5}$ | $9.9\times10^{-6}$ |
| G0.5 | $3.69\times10^{-8}$ | 0.337 | 0.265 | 0.195 | $1.32\times10^{6}$ | $8.4\times10^{-7}$ |
| G3 | $2.66\times10^{-9}$ | 0.403 | 0.271 | 0.183 | $1.78\times10^{7}$ | $6.1\times10^{-8}$ |
| G6 | $3.83\times10^{-8}$ | 0.371 | 0.271 | 0.195 | $1.28\times10^{6}$ | $8.7\times10^{-7}$ |

The electrochemical impedance spectrum of the TC4 sample in the etching solution is shown in Figure 4. From the enlarged part in the figure, the maximum radius of the capacitive reactance arc of 3g/L can be obtained, so the best resistance to ion corrosion is obtained, and each sample has only one capacitive reactance arc, and the sample has only one time constant. When the resistor is connected in parallel with the capacitor, the low frequency band in the Bode plot (|Z|-logf) is a horizontal line parallel to the horizontal axis, and the high frequency phase is a straight line with a slope of -1, so as shown in Figure 4. The equivalent circuit model shown in Figure 5 is used to fit the electrochemical impedance spectrum data [20,21], and the corresponding results are shown in Table 3. Corner elements (Q1 and n1 represent the electrolyte/coating interface, Q2 and n2 represent the inner and substrate interfaces) and resistive elements (Rs for solution, R1 for the loose layer and R2 for the dense layer) constitute the micro-arc oxide coating electrical components. R1 and R2 are improved due to the addition of graphene. The coating resistances R1 and R2 is up to $6.185\times10^{7}$ Ω/cm$^2$ and $8.503\times10^{4}$Ω/cm$^2$ respectively, when the graphene content is 3 g/L. CPE is a constant phase angle component. For non-ideal capacitors, CPE is used instead of electric double layer capacitor. The CPE value is related to the surface condition of the material, such as roughness, porosity, etc. And n represents the diffusion coefficient of the original phase angle original CPE, and the larger the value, the better the corrosion resistance. The dense layer is more resistant to ion corrosion. The coating containing 3 g/L of graphene particles has the largest value of n, which indicates that the corrosion resistance of the coating is improved due to the addition of graphene, and the optimum addition amount is 3 g/L.

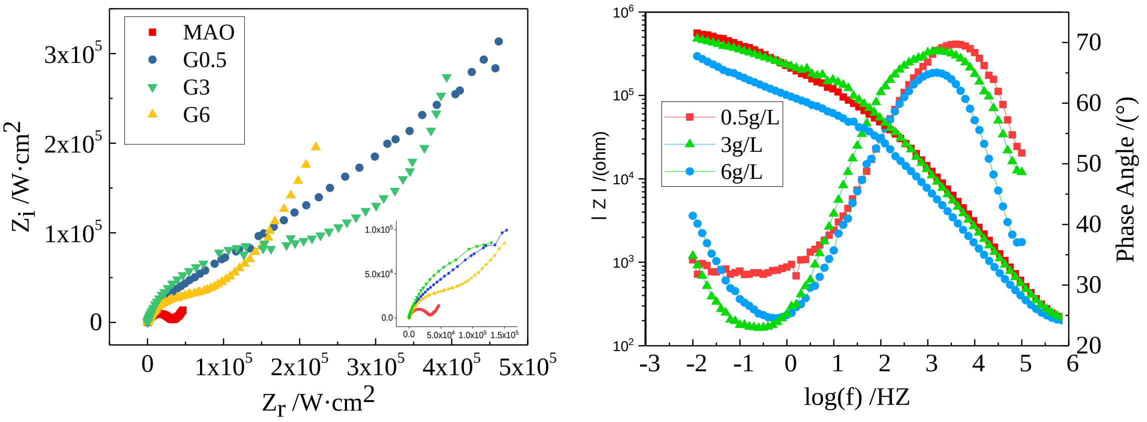

**Figure 4.** Influence of graphene concentration on Nyquist (a) and Bode (b) plots of samples in 3.5% sodium chloride solution

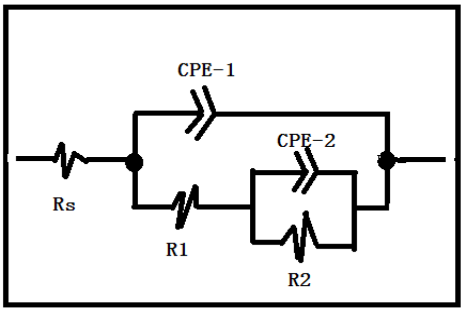

**Figure 5.** Equivalent circuit model used in the fitting of the impedance data for sample

**Table 3.** Electrical component parameters of the equivalent circuit

| Sample | Electrochemical parameters | | | | | | |
|---|---|---|---|---|---|---|---|
| | Rs (Ω/cm²) | CPE1 | | R1 (Ω/cm²) | CPE2 | | R2 (Ω/cm²) |
| | | Q1 (F/cm²) | n1 | | Q2 (F/cm²) | n2 | |
| G0 | 7.62 | $6.305\times10^{-7}$ | 0.599 | $4.585\times10^{7}$ | $4.012\times10^{-7}$ | 0.427 | $3.263\times10^{4}$ |
| G0.5 | 12.01 | $1.757\times10^{-7}$ | 0.694 | $5.219\times10^{7}$ | $2.351\times10^{-7}$ | 0.738 | $7.089\times10^{4}$ |
| G3 | 13.08 | $1.292\times10^{-7}$ | 0.797 | $6.185\times10^{7}$ | $1.004\times10^{-7}$ | 0.830 | $8.503\times10^{4}$ |
| G6 | 11.18 | $2.092\times10^{-7}$ | 0.791 | $5.813\times10^{7}$ | $2.069\times10^{-7}$ | 0.829 | $5.381\times10^{4}$ |

Since the graphene particles present in the electrolyte can adsorb electrons, under the action of a strong electric field, the molten oxide envelops the graphene into the discharge micropores, hinders the entry of the corrosive medium, and simultaneously generates SiC, so the values of Q1 and Q2 decrease. When the graphene is excessive in the electrolyte, the micro-arc oxidation reaction is severe, and micro-cracks appear on the surface, so that the corrosive ions enter the micropores, and the values of Q1 and Q2 increase.

### *3.3. Effect of graphene content on galvanic corrosion behavior of coating*

Figure 6 shows the variation of corrosion current and corrosion potential with time after the galvanic couple of different samples and S135 steel. It can be seen that both the corrosion current and potential gradually increases with time, and finally stabilizes. For the titanium alloy, the corrosion current finally stabilizes at about 0.96 mA, which is significantly higher than MAO coatings. It can be seen that as the graphene content increases, the corrosion current firstly decrease and then increase, the change of corrosion potential is just the opposite.

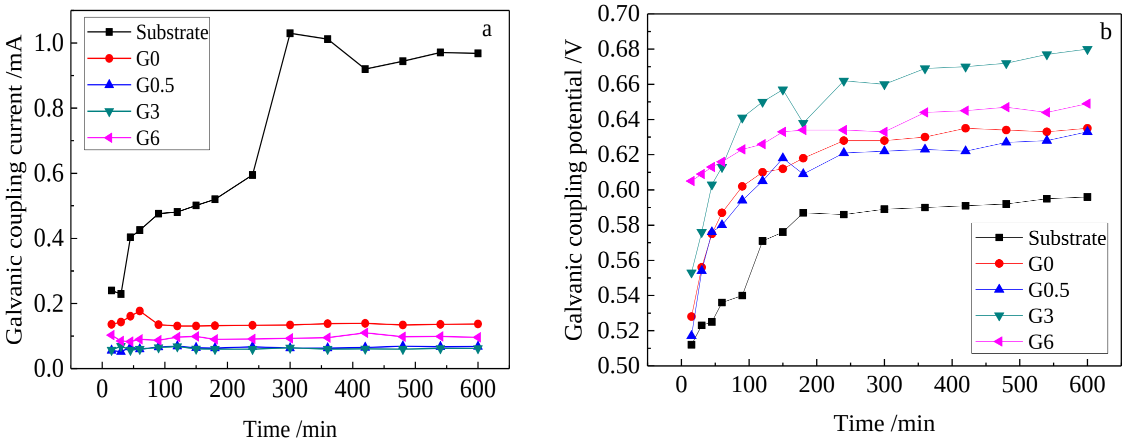

**Figure6.** the curve of corrosion current (a) and corrosion potential (b) with time after galvanic corrosion of different sample groups

**Table 4.** Corrosion morphology of galvanic corrosion with different galvanic couple samples

| **Samples**<br>**Material** | **TC4** | **G0** | **G0.5** | **G3** | **G6** |
|---|---|---|---|---|---|
| **Titanium alloy** |  |  |  |  |  |
| **S135** |  |  |  |  |  |

The corrosion current of G0 is about 0.13 mA, G0.5 and G3 are very similar, about 0.06 mA, and then the corrosion current increases to 0.1 mA as the graphene content increases. It can be seen from Fig. b that as time increases, the coupling potential gradually increases, and the fluctuation decreases after about 150 minutes, finally stabilizes. The coupling potential of the TC4 titanium alloy matrix is finally stabilized at about 0.59 V, which is lower than that of the micro-arc oxidation coating. The smaller the corrosion current and the greater the coupling potential of the galvanic corrosion, indicating that the galvanic corrosion resistance is better. After the micro-arc oxidation treatment of the titanium alloy substrate, a ceramic coating is formed on the surface, which greatly improves the resistance to contact corrosion. When graphene is added to the electrolyte, SiC is formed in the coating and a small amount of graphene is present, which further enhances the ability of the coating to resist contact corrosion.

Table 4 shows the corrosion morphology of the different micro-arc oxide film layers and the S135 couple pairs. There are investigations [10,22] found that TC4 not only has a high self-corrosion potential, but also has excellent corrosion resistance. Other metals are prone to galvanic corrosion when in contact, thereby accelerating the corrosion rate of metals with lower potentials. As can be seen from the chart, when the titanium alloy is coupled with the S135 steel, since the potential of the titanium alloy is higher than that of the S135 steel, the steel is firstly corroded. When S135 steel was coupled with TC4 titanium alloy matrix, S135 steel experienced severe corrosion, and almost the entire sample was covered by corrosion products. When the sample G0 coating coupled with S135 steel, the corrosion area of the S135 steel is less than half of the entire sample. As the graphene added in the electrolyte increases, the S135 steel coupled with coating is corroded slightly. When the graphene content is 3 g/L, the corrosion degree of S135 steel is the lightest, and only about 1/5 of the surface area is corroded. It can be found that the TC4 titanium alloy and the MAO coating samples were hardly corroded in the galvanic couple.

### *3.4. Analysis and discussion of corrosion mechanism*

The galvanic corrosion caused by different metal contacts must have three basic conditions [23]: a certain potential difference, the presence of corrosive electrolyte and electrical connection. The above conditions are constructed into an unstable electrolytic cell system. Electrochemical corrosion can be divided into hydrogen evolution corrosion and oxygen absorption corrosion. Under the experimental conditions, oxygen corrosion reaction occurs, and the cathode reduction process absorbs electrons generated by metal corrosion, causing the metal to suffer continuous corrosion. Related studies have shown that the distribution of galvanic corrosion current is closely related to the area ratio of the anode to the cathode, the distance between the anode and the cathode, the placement depth of the couple in the solution [24]. In the control sample of the galvanic corrosion test in this study, our only variable is the material of the galvanic pair.

As a surface protection measure, micro-arc oxidation can reduce the sensitivity of galvanic corrosion between titanium alloy and aluminum alloy and structural steel to a certain extent, but it cannot completely prevent it [25]. There are discharge micropores in the film structure, and the corrosive medium easily enters the inside of the film through the discharge holes, thereby causing corrosion. The corrosion resistance of the micro-arc oxidation coating is mainly affected by factors such as the number of micropores, pore size, film thickness and composition [26]. First of all, the thickness of the micro-arc oxide coating obtained by adding a certain amount of graphene to the electrolyte is significantly increased (in the case of G3, the coating thickness is increased by 183%), and the increase of the thickness of the coating plays an important role in improving the corrosion resistance. Secondly, the composition and structure of the micro-arc oxidation film changed after the addition of graphene. The main component of the film after micro-arc oxidation without addition of graphene is titanium oxide and a small amount of amorphous $SiO_2$, and after adding graphene, the film also contains SiC and a small amount of graphene. SiC and graphene are uniformly dispersed in the original coating. The high hardness of SiC, good toughness of graphene and film compactness all contribute to the improvement of the corrosion resistance of the coating.

## 4. CONCLUSION

In this work, the corrosion performance of TC4 titanium alloy matrix and MAO coating was compared by electrochemical experiments. Compared with S135 steel, titanium alloy has higher potential and excellent corrosion resistance. In the micro-arc oxidation, a part of the graphene particles formed a small amount of SiC in the coating under the action of the arc high temperature. In the electrochemical experiment, it was found that the corrosion current density was reduced to $2.66\times10^{-9}$ $A/cm^2$, and the coating with smallest corrosion coefficient when the additive amount of graphene was 3 g/L. The galvanic corrosion test show that the surface of TC4 titanium alloy after micro-arc oxidation treatment has a dense oxide coating with good stability and high electrical resistance, which can effectively stabilize and reduce the electric current. Therefore, the coupling of micro-arc oxide coating and S135 after the current pairing of the steel, the current density is significantly reduced. We can also draw conclusions that the micro-arc oxidation treatment can improve the surface corrosion resistance and reduce the galvanic corrosion sensitivity, and best addition amount of graphene in this experiment is 3g/L.

ACKNOWLEDGMENTS
The authors (Dr. Chen) thank for the financial support of National Natural Science Foundation Interview Project Funding (No: 51774249) and authors are also thankful to Southwest Petroleum University for providing the Sophisticated Instrumentation Facility to carrying out this research investigation.

## References

1. Y. Liu, Z. D. Qu and B. X. Wang, *Ordnance Mater. Sci. Eng.*, 28 (2005) 47.
2. H. Jiang and X. D. Zhang, *Adv. Mater. Ind.*, 3 (2017) 7.
3. X. Q. Ma, Z. T. Yu, J. L. Liu, S. Yu, S. H. Liu and X. J. He, *Nonferrous Metal Materials and Engineering*, 6 (2018) 26.
4. Y. X. Wang, C. T. Zhang and B. Zhang, *Oil Field Equip.*, 12 (2010) 31.
5. X. Y. Wu, H. Zhang, X. J. Xu, Z. S. Zhang and S. J. Guo, *Petrochem. Ind. Appl.*, 11 (2016) 105.
6. J. Zhao, S. A. Chen, Y. G. Liu and G. S. Li, *Oil Field Equip.*, 5 (2011) 96.
7. L. P. Qi, Y. Ding, Q. L. Liao and Y. Zhang, *Adv. Mater. Ind.*, 3 (2017) 35.
8. X. J. Xing, Y. N. Gen and H. Q. Feng, *Technology Supervision in Petroleum Industry*, 1 (2017) 46.
9. C. S. Wang, D. Z. Zeng, T. H. Shi, G. L. Cai, M. H. Zhang and Z. Tao, *China Sciencepap.*, 9 (2015) 999.
10. Y. F. Chen, Z. X. Li, L. T. Liu, H. N. Wang, Y. F. Wang and Y. F. Peng, *Rare Met. Mater. Eng.*, 4

(2019) 1161.
11. X. W. Chen, T. H. Shi, X. Jiang, D. F. Zhang, P. F. Zhao, X. P. Chen, L. P. Cai and W. X. Chen, *Mater. Prot.*, 10 (2018) 75.
12. S. Palani, A. Rose and K. Legg, Modeling galvanic corrosion behavior of carbon fiber composite/Al 7050 joints under extended exposures, 2017 Department of Defence Allied Nations Technical Corrosion Conference. Arizona, USA, 2017, PP. 1.
13. Darya Snihirova, Daniel Höche, Sviatlana Lamaka, Zahid Mira, Theo Hack and Mikhail L. Zheludkevich, *Corros. Sci.*, 157 (2019) 70.
14. Y. J. Yang, X. Y. Zhang and M. H. Liu, *J. Mater. Eng.*, 12 (2012) 55.
15. Y. J. Yang, X. Y. Zhang and M. H. Liu, *J. Aeronaut. Mater.*, 5 (2015) 57.
16. L. J. Chen, J. Y. Hu, X. K. Zhong, S. Y. Yu, Z. Zhang, D. Z. Zeng and T. H. Shi, *Int. J. Electrochem. Sci.*, 12 (2017) 9445.
17. P. Du, J. Z. Li, Y. L. Zhao, Y. G. Dai, Z. D. Yang and Y. W. Tian, *Int. J. Electrochem. Sci.*, 13 (2018) 11164.
18. X. W. Chen, D. D. Liao, D. F. Zhang, X. J, P. F. Zhao, and R. S. Xu, *Trans. Indian Inst. Met.,* 2019.
19. Hamid Reza Bakhsheshi-Rad, Majid Abdellahi, Esah Hamzah, Ahmad Fauzi Ismail and Maryam Bahmanpour, *J. Alloys Compd.*, 687 (2016) 630.
20. K. M. Ismail, A. M. Fathi and W. A. Badawy, *Corros. Sci.*, 8 (2006) 1912.
21. P. Bala Srinivasan, C. Blawert and W. Dietzel, *Corros. Sci.*, 50 (2008) 2415.
22. R.Winston Revie, *Uhlig,s Corrosion Handbook*, Chemical Industry Press, 2005, Beijing, China.
23. H. F. Zhang, *IOP Conf. Series: Earth and Environmental Science,* 225 (2019) 22015.
24. Y. J. Xu, *The Study on Galvanic Corrosion and Protection of Magnesium Alloys coupled with other alloys,* Chongqing University, 2010, Chongqing, China.
25. W. Y. Zhang, *Total Corrosion Control,* 32 (2018) 51.
26. B. Liu, *Preparation and Corrosion Properties of coating formed on LY12 Alloy by spraying Microarc Oxidation*, Harbin Institute of Technology, 2009, Harbin, China.

© 2020 The Authors. Published by ESG (www.electrochemsci.org). This article is an open access article distributed under the terms and conditions of the Creative Commons Attribution license (http://creativecommons.org/licenses/by/4.0/).